Available online at www.sciencedirect.com
ScienceDirect
Comput. Methods Appl. Mech. Engrg. 197 (2008) 2585–2595
Computer methods in applied mechanics and engineering
www.elsevier.com/locate/cma

A probabilistic construction of model validation

Roger G. Ghanem [a,*], Alireza Doostan [b], John Red-Horse [c]

[a] 210 KAP Hall, University of Southern California, Los Angeles, CA 90089, United States
[b] Stanford University, Department of Mechanical Engineering, Stanford, CA, United States
[c] Validation and Uncertainty Quantification Department, Sandia National Laboratories, MS0828, Albuquerque, NM 87185, United States

Received 19 June 2007; received in revised form 14 August 2007; accepted 14 August 2007
Available online 23 December 2007

Abstract

We describe a procedure to assess the predictive accuracy of process models subject to approximation error and uncertainty. The proposed approach is a functional analysis-based probabilistic approach for which we represent random quantities using polynomial chaos expansions (PCEs). The approach permits the formulation of the uncertainty assessment in validation, a significant component of the process, as a problem of approximation theory. It has two essential parts. First, a statistical procedure is implemented to calibrate uncertain parameters of the candidate model from experimental or model-based measurements. Such a calibration technique employs PCEs to represent the inherent uncertainty of the model parameters. Based on the asymptotic behavior of the statistical parameter estimator, the associated PCE coefficients are then characterized as independent random quantities to represent epistemic uncertainty due to lack of information. Second, a simple hypothesis test is implemented to explore the validation of the computational model assumed for the physics of the problem. The above validation path is implemented for the case of dynamical system validation challenge exercise.

Keywords: Model validation; Uncertainty quantification; Maximum likelihood

1. Introduction

In the world of modeling and simulation, two stark realities exist. First, all models are approximations of their target phenomena; and second, uncertainties exist, due both to ignorance and poorly understood inherent processes, that corrupt our ability to state with certainty the level of approximation that is present in them. Historically, these so-called epistemic and aleatory uncertainties, respectively, have been handled through ad hoc means by using such mechanisms as safety factor-based margins in design and qualification of systems. The precise values for a given safety factor are application specific, and typically involve years of experience to adjust.

Thus, in this era of heightened hopes and expectations for expanding the use of modeling and simulation in many areas of science and engineering, including those with significant risks that can be attributed to system failure scenarios, comes the need to develop means to assess the predictive capabilities of a given model. This exercise has come to be known as model validation, and it is critical, given the underlying constraints, that model validation entails procedures to accommodate concomitant error and uncertainty.

There are distinct components associated with any predictive process. One must first establish a context; and, within this context, build a model; then one uses this model to achieve their result. When this process is mathematical in nature, the first step entails identifying meaningful physical constraints on a quantity of interest, and using these to formulate a governing set of equations. A functional space approach has proved useful for representing these constraints. With them, one can develop functional relationships that approximate observed behaviors such as mass conservation, boundary conditions, and sources of significant energy contributions, along with necessary mathemat-

* Corresponding author. Tel.: +1 213 740 9528; fax: +1 213 740 2037.
E-mail addresses: ghanem@usc.edu (R.G. Ghanem), doostan@stanford.edu (A. Doostan), jrredho@sandia.gov (J. Red-Horse).

0045-7825/$ - see front matter © 2007 Elsevier B.V. All rights reserved.
doi:10.1016/j.cma.2007.08.029

ical constraints, such as smoothness, and appropriate restrictions on domains of definition. Together these conditions produce a well-posed, regularized mathematical model capable of rendering well-behaved solutions.

Accommodating uncertainty requires a change of context. We propose a probabilistic framework for this; and, within this framework, we proffer a functional analytic approach to probability. In this way we can retain the same functional space constructions that we use for a deterministic process. Specifically, the measure with respect to which all the norms are defined is now constructed as the product measure based on the original deterministic measure combined with a suitable probabilistic measure. Any uncertainty model is phenomenologically driven, and the probabilistic measure we employ should capture effects present in the available experimental evidence. A significant feature of our approach is that we can now refine the outcome of this first analysis stage either by changing the selection of physical phenomena captured in the definition of the functional spaces, or by changing the probability measure to reflect a change in the underlying evidence.

The second step in the predictive process involves obtaining a solution using the above context and model. We note that the functional space construction is preserved under a probabilistic approach to uncertainty, and that the body of approximation theory developed traditionally for deterministic problems is readily adapted to accommodate uncertainty. Thus, numerical approximation to the solution of the governing equations that rely on topological and algebraic properties such as norm minimization, orthogonal projections, and fixed point theorems are all inherited from deterministic analysis. With this mathematical structure, the question of model validation can be cast as a problem in approximation theory providing, in addition to whether a model is valid or not, *a posteriori* indicators that are useful for, among other things, the allocation of resources aimed at further validating a given model.

Implicit in most uncertainty quantification schemes is the assumption that the parameters in the governing equations have been accurately characterized as probabilistic entities, such as random variables (RVs), or random fields (RFs), the latter of which are often referred to as stochastic processes. Our approach is to cast these entities in a functional analytic context using generalized Fourier expansions. In particular, we use Polynomial Chaos expansions (PCEs) [14,11,10,13,12,29,16,18,17,5], defined in Hilbert spaces [24,46] to represent the random entities, and leverage our experience with deterministic systems taken in this same context to develop solution procedures based on PCEs. From the viewpoint of input/output, this process can be viewed as an efficient means to propagate the probabilistic information regarding the system parameters to the solution.

In the preceding text, we have stated our motivation for developing a modeling framework that is useful for augmenting a deterministic analysis to enable simultaneous uncertainty evaluation. The astute reader will notice that this framework is itself a modeling context that is subject to its own epistemic limitations. For example, it is rarely possible to acquire enough data on particular system parameters to achieve a fully precise probabilistic characterization. When this uncertainty becomes important, it, too, must be factored into our new analysis framework. Fortunately, our approach, based on generalized Fourier expansions, provides a unique capability. Strategies for choosing the expansion order based on contributions to the overall error are possible. Moreover, we can view the sensitivity of the system parameters to additional information as a perturbation of their Fourier coefficients. The impact of expansion length and of these perturbations has the effect of refining the probabilistic measure of the data and the predictive capability of the mathematical model. Research on the Fourier coefficient perturbation has used maximum-likelihood, [6] and Bayesian [15] arguments to compute estimates of the PCE coefficients of parameters from associated statistical samples. In the present work the application guides us to adapt the maximum-likelihood framework for representation of parameter uncertainty to the dynamical system validation challenge exercise. The benefit of this approach lies in the ability to characterize both the epistemic and aleatory uncertainties of model parameters. It is worth mentioning that the present approach relaxes some restrictive assumptions of current procedures [2,19] for characterizing the random parameters of a stochastic system from limited data, in the sense that no particular form for the underlying random parameter is assumed.

The paper is organized as follows. In Section 2, we provide a detailed description of the proposed uncertainty representation procedure. Then, we briefly overview two schemes for effecting the uncertainty propagation in Section 3. Following that, we describe the choice of the validation metric for the particular application that is the subject of this work in Section 4. Finally, the results of the proposed validation analysis of the dynamical system challenge exercise are illustrated in Section 5.

2. Representation of random coefficients

Let $a(x,\omega) : \mathscr{D} \times \Omega \to \mathbb{R}$ denote the random field used to mathematically describe model parameters synthesized from available experimental data. Here $\mathscr{D}$ is an open, bounded polygonal domain in $\mathbb{R}^d$ and is the spatial domain on which a is defined, Ω is the set of elementary events on which a probability space is constructed. It is well known that $a(x,\omega)$ can be efficiently represented using the spectral decomposition of its corresponding two-point correlation function [27]. Let $\boldsymbol{a}_1, \boldsymbol{a}_2, \ldots, \boldsymbol{a}_M$ be M real row vectors in $\mathbb{R}^N$ representing M independent observations from random vector $\boldsymbol{a}(\omega) := (a(x_1,\omega), \ldots, a(x_N,\omega))$, and let $\boldsymbol{C}$ be the associated covariance matrix of $\boldsymbol{a}$. Finally, let $\boldsymbol{\Xi}$ denote the set of observation points $x_1, \ldots, x_N$, so that, $\boldsymbol{\Xi} = \{x_i \in \mathscr{D}, i = 1, \ldots, N\}$.

We need to get our information into a format that is amenable to accommodating the various uncertainties

manifested in the measurement data. We begin by computing the well-known unbiased statistical estimators for the mean and covariance of the random vector $\boldsymbol{a}(\omega)$. These expressions are $\bar{\boldsymbol{a}} = \frac{1}{M}\sum_{i=1}^{M}\boldsymbol{a}_i$ and

$$\widehat{\mathbf{C}} = \frac{1}{M-1}\sum_{i=1}^{M}(\boldsymbol{a}_i - \bar{\boldsymbol{a}})^{\mathrm{T}}(\boldsymbol{a}_i - \bar{\boldsymbol{a}}), \tag{1}$$

respectively. Next, we decompose $\widehat{\mathbf{C}}$ using the Karhunen–Loève (KL) procedure [27], and construct the following representation of $\boldsymbol{a}$

$$\boldsymbol{a}(\omega) = \bar{\boldsymbol{a}} + \sum_{i=1}^{N}\sqrt{\lambda_i}\eta^{(i)}(\omega)\boldsymbol{\phi}_i. \tag{2}$$

Here, $\{\lambda_i\}_{i=1}^{N}$ and $\{\boldsymbol{\phi}_i\}_{i=1}^{N}$ are the eigenvalues and eigenvectors of $\widehat{\mathbf{C}}$, respectively.

We then use the relative magnitude of the KL eigenvalues to obtain a reduced-order representation of $\boldsymbol{a}(\omega)$. That is, we establish μ by requiring that $\sum_{i=1}^{\mu}\lambda_i/\sum_{i=1}^{N}\lambda_i$ is sufficiently close to one, and arrive at the following approximation:

$$\boldsymbol{a}(\omega) \approx \bar{\boldsymbol{a}} + \sum_{i=1}^{\mu}\sqrt{\lambda_i}\eta^{(i)}(\omega)\boldsymbol{\phi}_i. \tag{3}$$

In Eq. (2), the $\eta^{(i)}$, $i = 1,\ldots,N$ are uncorrelated random variables. For these μ random variables, we can readily obtain sample realizations from the original data and the KL relationship as follows:

$$\eta_j^{(i)} = \frac{1}{\sqrt{\lambda_i}}\langle \boldsymbol{a}_j - \bar{\boldsymbol{a}}, \boldsymbol{\phi}_i\rangle_{l_2}, \quad j = 1,\ldots,M, \tag{4}$$

where $\langle\cdot,\cdot\rangle_{l_2}$ denotes the usual scalar product in $\mathbb{R}^N$.

Finally, based on Eq. (3), the components of the random vector, $\boldsymbol{\eta} := (\eta^{(1)}\ldots\eta^{(\mu)})$, have the following two properties:

$$E[\eta^{(n)}] = 0, \quad E[\eta^{(m)}\eta^{(n)}] = \delta_{mn}, \quad n,m = 1,\ldots,\mu, \tag{5}$$

where

$$\delta_{mn} = \begin{cases} 1, & m = n, \\ 0, & \text{otherwise.} \end{cases} \tag{6}$$

Note that $\boldsymbol{\eta}$ is composed of uncorrelated, generally statistically dependent random variables about which we know only the information reflected in the available measurement data. Having only limited observations from $\boldsymbol{\eta}$, we almost certainly lack sufficient information to establish a probabilistic model for it, such as, say, a joint cumulative distribution function. Since the underlying random field $a(x,\omega)$ is, in general, not Gaussian, the random variables $\eta^{(i)}$ are also generally non-Gaussian. Thus the problem reflects so-called epistemic uncertainty, and a means must be effected that addresses this while properly accounting for system uncertainty that is consistent with the known information.

In the sequel, we will use function approximation methods as a means to construct implicit parameterizations of $\boldsymbol{\eta}$ with statistically independent components that retain as much information as is practical, and can be justified, from the data and the problem specification. That is, we will construct a dependent, non-Gaussian random μ-vector, $\widehat{\boldsymbol{\eta}}$, such that $\widehat{\boldsymbol{\eta}}$ and $\boldsymbol{\eta}$ have identical covariance matrices, $\mathbf{I}_{\mu\times\mu}$.

Relaxing this assumption to account for dependence presents no theoretical difficulties; however, it does present a number of computational and experimental challenges [6]. Also, methods have been proposed that are designed specifically to analyze systems with various forms of epistemic uncertainty [37]. While any of these could have been used here, we have elected to follow a simpler procedure to emphasize the important features of the function approximation scheme.

Throughout this article, we have assumed that the mean and the dominant eigenspace of the estimated covariance matrix, $\widehat{\boldsymbol{C}}$, are invariant under a sequence of rank one perturbations associated with the assimilation of additional measurements. This assumption guides our use of the KL eigenvectors and eigenvalues that are obtained from the initial measurements in our analysis. Note that this assumption can also readily be relaxed by recomputing the dominant subspace as additional observations are obtained.

2.1. Function approximation for $\eta^{(i)}$

We briefly mentioned our intention to model uncertainties in the context of function approximation in Hilbert Space. Here we provide the details of the process, which are given in terms of polynomial chaos expansions (PCEs).

To begin, we remark that it is always possible to establish a mapping between a given random variable and a Gaussian random variable, given the marginal cumulative distribution function of $\hat{\eta}^{(i)}$, where the equivalence is understood to be *in distribution*. More specifically, for each $i = 1,\ldots,\mu$, let $F_{\eta^{(i)}}$ denote the marginal cumulative distribution function of $\eta^{(i)}$, then $\hat{\eta}^{(i)} \sim F^{-1}_{\eta^{(i)}}(\Phi(\xi_i))$ with $\Phi(\xi_i) = \int_{-\infty}^{\xi_i}\frac{1}{\sqrt{2\pi}}\mathrm{e}^{\left(-\frac{z^2}{2}\right)}\mathrm{d}z$ and $\xi_1,\ldots,\xi_\mu$ are independent standard normal random variables.

In our mathematical setting, we can also express these mappings as generalized Fourier expansions with one-dimensional normalized Hermite polynomials in ξ_i serving as the basis functions [40,36]. This results in

$$\hat{\eta}^{(i)} = \sum_{j=1}^{\infty}\gamma_j^{(i)}\bar{\psi}_j(\xi_i) \approx \sum_{j=1}^{p_i}\gamma_j^{(i)}\bar{\psi}_j(\xi_i), \quad i = 1,\ldots,\mu, \tag{7}$$

where

$$\bar{\psi}_j(\xi_i) := \psi_j(\xi_i)\Big/\left(E\left[\psi_j^2(\xi_i)\right]\right)^{1/2} \tag{8}$$

and

$$\begin{aligned} &\psi_0(\xi_i) = 1, \\ &\psi_1(\xi_i) = \xi_i, \\ &\psi_{j+1}(\xi_i) = \xi_i\psi_j(\xi_i) - j\psi_{j-1}(\xi_i) \end{aligned} \tag{9}$$

are the non-normalized Hermite polynomials in ξ_i [1], and finally

$$E\left[\psi_j^2(\xi_i)\right] = \frac{1}{\sqrt{2\pi}} \int_{-\infty}^{+\infty} \psi_j^2(\xi_i) \mathrm{e}^{\left(-\frac{\xi_i^2}{2}\right)} \mathrm{d}\xi_i. \tag{10}$$

Appropriate values for p_i depend on a number of factors, including, most importantly, the need to meet a error threshold in the approximation. For cases where a large value of p_i is required to accurately represent each $\hat{\eta}^{(i)}$, e.g. when the random variables follow a distribution that is identified as multi-modal [45], the above representation and, accordingly, the subsequent procedures may be inefficient in their current format. Regardless, a key point to remember is that once the stochastic dimension, μ, and expansion order p_i have been set in a given expansion, the model form of the now implicitly defined marginal probability distribution for $\hat{\eta}^{(i)}$ is set as well. Owing to the availability of such methods, and their core dependence on basic propagation techniques, we have elected to focus only on the latter process here.

In closing, we comment on the mathematical framework within which we are operating as we use PCEs.

Many orthogonal polynomials derive from particular ordinary differential equations defined on Hilbert spaces [46] known as Sturm–Liouville systems. These systems induce an associated inner product weighting function that defines their orthogonality properties. For the Hermite polynomials this weighting function is, to within a constant, readily recognized to be the probability density function of a standard normal RV, which explains our choice above.

There are a couple of analytical benefits that follow immediately. First, for the discrete case it is possible to generalize to higher dimensions in $\hat{\eta}^{(i)}$. We caution, though, that the process is rather complicated; we refer the reader to [18] for the details.

Secondly, there are a number of other known probability density functions that also can be identified, simply by inspection, as weighting functions for inner products from different Sturm–Liouville systems. For example, an exponentially distributed RV defined on the interval $[0,\infty)$, can be seen to be affiliated with the Laguerre polynomials. Note that none of the underlying theory, nor the operations necessary for constructing the associated generalized Fourier expansions rely on a particular RV/orthogonal polynomial pairing. Thus, theoretically, it is possible that PCEs can be generalized to any appropriate pairing. These generalizations, often termed Askey Expansions in the literature, are the subject of active research [44,3,25,26].

2.2. Maximum likelihood formulation

As indicated previously, the present construction yields the components of a random vector for which the marginal distributions, $F_{\eta^{(i)}}$, cannot be approximated properly. Therefore, the true coefficients, $\gamma_j^{(i)}$, cannot be obtained by already available techniques [36,40]. In this section, we describe a novel approach, that relies on Maximum Likelihood parameter estimation, to characterize them. Clearly, once we have a statistical estimate of $\gamma_j^{(i)}$, the stochastic function $a(x,\omega)$ can be reconstructed by simply replacing $\boldsymbol{\eta}$ with $\widehat{\boldsymbol{\eta}}$ in the representation of a

$$\hat{\boldsymbol{a}}(\omega) = \bar{\boldsymbol{a}} + \sum_{i=1}^{\mu} \sqrt{\lambda_i} \hat{\eta}^{(i)}(\omega) \boldsymbol{\phi}_i. \tag{11}$$

Depending on the desirable degree of smoothness of a on $\mathscr{D}$, one might replace $\boldsymbol{\phi}_i$ and $\bar{\boldsymbol{a}}$ with their suitable interpolants in order to have a representation of a on any point inside $\mathscr{D}$.

The maximum likelihood estimation (MLE) framework provides a robust procedure for estimating the unknown coefficients $\gamma_j^{(i)}$ in the PCE of Eq. (7) from the independent, identically distributed (iid) observations $\boldsymbol{\eta}_1, \ldots, \boldsymbol{\eta}_M$.

The likelihood function for independent observations $\eta_1^{(k)}, \ldots, \eta_M^{(k)}$ from $\eta^{(k)}$ is defined as

$$L(\boldsymbol{\gamma}) := \prod_{j=1}^{M} p_{\hat{\eta}^{(k)}}(\eta_j^{(k)}|\boldsymbol{\gamma}), \tag{12}$$

where $p_{\hat{\eta}^{(k)}}(\eta_j^{(k)}|\boldsymbol{\gamma})$ is the marginal conditional probability density function (pdf) of $\eta^{(k)}$ given $\boldsymbol{\gamma}$.

We define $\boldsymbol{\gamma}_0 := (\gamma_1^{(k)}, \ldots, \gamma_p^{(k)}) \in \boldsymbol{\Lambda}$ to be the true value of the coefficients in the PCE for $\eta^{(k)}$. Elements of $\boldsymbol{\Lambda}$ must be constructed to satisfy Eq. (5), which means that

$$\sum_{j=1}^{p_i} (\gamma_j^{(i)})^2 = 1, \quad i = 1, \ldots, \mu. \tag{13}$$

An element of this type resides in a so-called *Hatcher02* manifold $\mathscr{O}(p,1)$ [21]. We specify $\hat{\boldsymbol{\gamma}} = (\hat{\gamma}_1^{(k)}, \ldots, \hat{\gamma}_{p_i}^{(k)}) \in \boldsymbol{\Lambda}$ to be its corresponding MLE estimate. By definition, $\hat{\boldsymbol{\gamma}}$ maximizes the likelihood function, Eq. (12), that is,

$$\hat{\boldsymbol{\gamma}} = \arg\max_{\boldsymbol{\gamma} \in \boldsymbol{\Lambda}} L(\boldsymbol{\gamma}). \tag{14}$$

Again, $\eta_1^{(k)}, \ldots, \eta_M^{(k)}$ are the M observations of $\eta^{(k)}$. These observations are also assumed to correspond to those of $\hat{\eta}^{(k)}$.

To avoid both the need for gradients and the computational cost associated with the constraint of Eq. (13), we effected our optimization problem using the method of simulated annealing (SA).

2.2.1. Simulated annealing

Simulated annealing (SA) is a stochastic algorithm for global optimization that is particularly well suited to problems with a large search space [23,4]. At each step of the algorithm, the current state, a sample point in the parameter space, is replaced by a point in a random *neighborhood* with a probability that depends on the difference between the corresponding values of the objective function and a parameter T. T is referred to as the *temperature*, which is reduced as the algorithm iterations increase. Early in the search, while T is at its largest, new candidate states that

are far from the current state are considered. This property mitigates tendencies to converge to local optima.

We now outline the SA algorithm we used to obtain $\hat{\gamma}$, which is the solution of Eq. (14), as follows [42]:

First, we define the objective function as $-L(\gamma)$, where $L(\cdot)$ was defined in Eq. (12).

(1) Set an initial temperature T and $\gamma_{\text{curr}} = \gamma_{\text{zero}} \in \Lambda$, calculate $L(\gamma_{\text{curr}})$.
(2) Randomly perturb γ_{curr} to get $\gamma_{\text{new}} \in \Lambda$ and calculate $L(\gamma_{\text{new}})$.
(3) Set $\delta = L(\gamma_{\text{new}}) - L(\gamma_{\text{curr}})$,
If $\delta \leqslant 0$ then move to γ_{new}.
If $\delta > 0$ then move to γ_{new} with probability $\exp(-\frac{\delta}{T})$.
(4) Repeat steps 2–3 sufficiently large. Lower T according to some annealing law (e.g. with rate $r_a = 1/\log i$ and i being the iteration index).
(5) Repeat steps 2–5 until convergence.

Remark 1. The states γ_{new} can be generated uniformly on $\mathcal{O}(p,1)$ and in a neighborhood of γ_{curr} based on the algorithm of [8].

Remark 2. In the above procedure, one needs to estimate the likelihood function, Eq. (12). A naive approach would be to sample the chaos basis and evaluate the likelihood at each $\eta_j^{(k)}$. Alternatively, one could obtain the likelihood function of single observation $\eta_j^{(k)}$, i.e. $p_{\hat{\eta}^{(k)}}(\eta_j^{(k)}|\gamma)$, by transforming the probability density function of a standard normal random variable based on the mapping (7), [34]. More specifically, let the mapping (7) be defined as $\hat{\eta}^{(i)} = g(\xi_i) := \sum_{j=1}^{p} \gamma_j^{(i)} \bar{\psi}_j(\xi_i)$ and let $\mathcal{S} = \{\xi_i^{(k)} \in \mathbb{R} : \hat{\eta}^{(k)} = g(\xi_i^{(k)})\}$ be the set of real roots of equation $g(\xi_i) - \hat{\eta}^{(i)} = 0$. Then $p_{\hat{\eta}^{(k)}}(\eta_j^{(k)}|\gamma)$ can be obtained from

$$p_{\hat{\eta}^{(k)}}(\eta_j^{(k)}|\gamma) = \sum_{\xi_i^{(k)} \in \mathcal{S}} \frac{\frac{1}{\sqrt{2\pi}} \exp(-(\xi_i^{(k)})^2/2)}{\left|\frac{\mathrm{d}g}{\mathrm{d}\xi_i}\Big|_{\xi_i^{(k)}}\right|}. \tag{15}$$

2.3. Representation of epistemic uncertainty

The MLE estimate, $\hat{\gamma}$, is a function of $\eta_1^{(k)}, \ldots, \eta_M^{(k)}$, and thus, for a finite M, varies with the observation set. We now investigate the performance of the estimator relative to these observations. We could do this by estimating the standard error, or confidence intervals, in the parameter estimates using resampling techniques (e.g. Bootstrap or Jackknife) when the estimate is computationally inexpensive [20,43]. Alternatively, we could rely upon large sample asymptotic behavior of the estimator, when it exists, to approximate its behavior. In the present work, for moderate values of p_i, the estimate $\hat{\gamma}$ is computationally cost prohibitive, thus motivating us to take the latter approach to assessing the variability of the PCE coefficient estimates, (7).

Under some regularity conditions, the fundamental result from the asymptotic, large-sample, MLE is that as more data is assimilated, the MLE estimate of the parameter vector approaches a multivariate normal distribution [9,35]. This result is stated in the following theorem.

Theorem 1 ([9,35]). *Under some regularity conditions (notably that the likelihood is a continuous function of γ and the true vector of parameters γ_0 not be on the boundary of the set to which γ belongs), as $M \to \infty$, the MLE estimate $\hat{\gamma}$ approaches normality with mean γ_0 and covariance matrix $(MJ(\gamma_0))^{-1}$, where J is the Fisher information matrix. In other words*

$$\sqrt{M}(\hat{\gamma} - \gamma_0) \xrightarrow{\text{dist}} N(0, J(\gamma_0)^{-1}). \tag{16}$$

In practice, for M reasonably large, $\hat{\gamma}$ is approximately $N(\gamma, (MJ(\gamma))^{-1})$ distributed when γ is chosen close to the unknown γ_0. Moreover, γ is usually approximated by $\hat{\gamma}$ for the mean and also for evaluation of the Fisher information matrix $J(\gamma)$ [42,9]. An important corollary of the above theorem is that $\hat{\gamma}$, is a *consistent* estimate for γ_0; that is, $\hat{\gamma}$ converges in probability to γ_0 as $M \to \infty$.

To characterize the complete probabilistic behavior of γ, one must develop procedures for evaluating the Fisher information matrix, $J(\hat{\gamma})$.

2.3.1. Estimation of the fisher information

Under suitable regularity conditions, the Fisher information matrix associated with the vector γ under the likelihood $p_{\hat{\eta}^{(k)}}(\hat{\eta}^{(k)}|\gamma)$ is defined as

$$J(\gamma) = -E\left[\frac{\partial^2 l(\gamma)}{\partial\gamma\partial\gamma^{\mathrm{T}}}\right] = E\left[\frac{\partial l(\gamma)}{\partial\gamma}\frac{\partial l(\gamma)^{\mathrm{T}}}{\partial\gamma}\right], \tag{17}$$

where $l(\gamma)$ is the log-likelihood of the data. In situations, including the present work, where the closed form of the likelihood is not available, the Fisher information cannot be computed analytically and thus has to be numerically approximated. For *i.i.d.* cases this approximation can be achieved using the so called *empirical Fisher information* $\hat{J}(\gamma)$ defined by [31,30,41]

$$\hat{J}(\gamma) = \sum_{i=1}^{M} \mathbf{s}_i(\gamma)\mathbf{s}_i(\gamma)^{\mathrm{T}} - \frac{1}{M}\left(\sum_{i=1}^{M}\mathbf{s}_i(\gamma)\right)\left(\sum_{i=1}^{M}\mathbf{s}_i(\gamma)\right)^{\mathrm{T}}, \tag{18}$$

where $\mathbf{s}_i(\gamma) = \frac{\partial l_i(\gamma)}{\partial\gamma}\Big|_{\hat{\eta}^{(k)}=\hat{\eta}_i^{(k)}}$ is the derivative of the individual log-likelihood evaluated at $\hat{\eta}_i^{(k)}$ and is called the *score* function. While being a *consistent* estimator of $J(\gamma)$, $\hat{J}(\gamma)$ is obtained by a simple finite difference scheme for the estimation of score functions. In summary, we state the approximate asymptotic behavior of the Maximum Likelihood estimates of the PCE coefficients as

$$\sqrt{M}(\hat{\gamma} - \gamma_0) \xrightarrow{\text{dist}} N(0, \hat{J}(\hat{\gamma})^{-1}). \tag{19}$$

2.4. Uncertainty modeling for the system parameter

Following the above probabilistic representation of the chaos coefficients, one can reconstruct each random variable $\hat{\eta}^{(i)}$ simply by replacing $\hat{\gamma}_j^{(i)}$ with $\tilde{\gamma}_j^{(i)}$ where, for each i, $\tilde{\gamma}_j^{(i)}$ are jointly Gaussian random variables with mean $\hat{\gamma}_j^{(i)}$ and covariance matrix $(M\hat{J}(\hat{\gamma}))^{-1}$ and are independent from $\{\xi_i\}_{i=1}^{\mu}$, i.e.

$$\hat{\eta}^{(i)} = \sum_{j=1}^{p} \tilde{\gamma}_j^{(i)} \bar{\psi}_j(\xi_i). \tag{20}$$

One obtains the final representation of $\hat{a}$ by substituting Eq. (20) into Eq. (11)

$$\hat{\boldsymbol{a}} = \bar{\boldsymbol{a}} + \sum_{i=1}^{\mu} \sqrt{\lambda_i} \left(\sum_{j=1}^{p_i} \tilde{\gamma}_j^{(i)} \bar{\psi}_j(\xi_i) \right) \boldsymbol{\phi}_i, \tag{21}$$

where it is worth noting that for different indices i, the random vectors $\tilde{\boldsymbol{\gamma}}^{(i)} := [\tilde{\gamma}_1^{(i)}, \ldots, \tilde{\gamma}_{p_i}^{(i)}]$ are mutually independent.

In the present section, we provided a detailed discussion of the mathematical elements on which we have based our procedure. During that discussion, we hinted at a significant feature, which we state here explicitly: Using our procedure, one is able to identify exactly where the two contributors of uncertainty, inherent and ignorance, reside in the probabilistic model. In the specific case of Eq. (21), the $\{\xi_i\}$ represent the stochastic dimensions necessary to capture the inherent uncertainty of $\hat{a}$. The $\{\tilde{\gamma}_j^{(i)}\}$ capture the ignorance-based uncertainty, which we have assumed here to be dominated by the lack of data in the estimation of the true parameters. The uncertainty due to physics modeling uncertainty, which is also ignorance based, and thus also captured in these terms, could readily be handled as well through a modeling change by increasing their underlying stochastic dimensions. We have elected to ignore this here due to its relatively small affect on the hypothesis test results discussed in Section 4 below.

Finally, approximation (21) originated from measurements that are assumed to be defined over a finite subset of the problem's physical domain. This is quite general, however. Not only can we extend our approximation to the entire domain $\mathscr{D}$ using suitable interpolation functions, e.g. Lagrange interpolation, Radial Basis Functions, or B-Spline, but the process works quite naturally for random vectors containing a finite number of parameters. The latter case is, in fact, applicable to the subject problem, where the first step naturally accounts for parametric correlation.

The accuracy of the proposed scheme for reconstruction of random fields based on their limited observation has been explored and verified in [15] for the case of a computational Bayesian estimator. Many of these properties are expected to hold for the Maximum Likelihood estimation used in the present work.

3. Uncertainty propagation

Since the quantities of interest are usually at the response level, there is a need to propagate the model parameter uncertainty, obtained from the procedures of Section 2, through the mathematical model to obtain probabilistic descriptions for response quantities of interest. As shown in [15], the uncertainty formalism of Section 2 is particularly well adapted to the case of stochastic Galerkin schemes. A very important advantage of the latter technique is the fact that one can investigate the sensitivity of the statistics of the quantity of interest with respect to impact of additional data, e.g. with respect to the variance of the random variables $\tilde{\gamma}_j^{(i)}$ of (27). We adopt a Monte Carlo simulation approach for uncertainty propagation in the analysis of Section 5, to comply with the requirements of the challenge problem.

4. Computation–observation comparison and the validation metric

The purpose of the present stage of model validation is to assess the quality of agreement between the model predictions and experimental data. Clearly, this comparison can only be carried out in relation to a specific quantity of interest (QOI). A number of *validation metrics*, [32,7,39], have been proposed in the literature to measure the distance between model predictions and experimental evidence.

In general, the choice of validation metric will depend on the problem under investigation. The most elementary validation metric is the *visual metric* where the analyst visually compares the graphs of computed response with those of experimental observations. Such a metric is purely qualitative and cannot properly accommodate the effects of uncertainty. Two other alternative *quantitative* metrics, are variations on *hypothesis testing*-based validation metrics, and consist of classical hypothesis testing or Bayesian hypothesis testing-based [22,33,47,28], which generally accept or reject the model based on some error statistics.

In the present work, the classical hypothesis testing-based validation technique is adopted to compare predictions of the quantity of interest, given the computational model, to the corresponding experimental observations. This approach entails testing a null hypothesis

$$H_0 : \hat{Q} = Q^{\mathrm{o}}, \tag{22}$$

where $\hat{Q}$ and Q^{o} are the computed quantity of interest, Q, based on the calibrated computational model and the corresponding experimental observation, respectively. Assuming a significance level α_s, e.g. we have taken $\alpha_s = 0.05$ here, if the experimental observation Q^{o} falls outside the two tail confidence regions having probability $1 - \alpha_s$ obtained from probability distribution function of $\hat{Q}$, which we obtain from the propagation analysis of Section 3, then the null hypothesis is rejected. Otherwise, there will be no evidence

to reject the hypothesis. In this hypothesis test, the underlying validation metric is implicitly defined as

$$d = |\hat{Q} - Q^o|. \tag{23}$$

Fig. 1 depicts a schematic description of above cases.

The above hypothesis test is repeated for all available observations and the candidate computational model will be rejected with a significance level α_{gs}, here $\alpha_{gs} = 0.10$, if more than $100 \times \alpha_{gs}$ percent of the tests are rejected. Otherwise, there is not enough evidence to reject the candidate computational model.

We emphasize that those observations used in the validation process should not correspond to the data used in the calibration process. The calibration process is defined to minimize, in some sense, the discrepancy between computed model responses and the calibration observations.

5. Statement of the validation problem

5.1. Target application

The problem of interest, as shown in Fig. 2, is a virtual dynamical system consisting of a beam with varying cross section properties on an elastic foundation and a three degree of freedom subsystem. The connection to the beam is weakly nonlinear and the analytical description of this nonlinearity is unknown and reflected only through the data. The *quantity of interest* is the probability of the maximum acceleration of the top mass in the subsystem exceeding some threshold under a shock load and is required to be below a specified threshold,

$$\text{Prob}\left\{\max_{t>0} |a(t)| > 1.8(10^4)\ \text{in/sec}^2\right\} < 10^{-2}. \tag{24}$$

The main objective will be to investigate whether or not the linear model is a valid model for prediction. Once a validated model is in hand, one can easily verify whether the system complies with the above design criterion, Eq. (24).

5.2. Subsystem calibration

As depicted in Fig. 3, the subsystem consists of a three degree of freedom system whose mechanical properties, e.g. masses, springs, and dampers, have inherent variabilities, aleatory uncertainty, and are to be calibrated based on limited virtual experiments thus exhibiting epistemic uncertainty. Therefore, any calibration procedure should suitably accommodate these two sources of uncertainty.

For the sake of calibration, 20 nominally identical structures, as in Fig. 3, are virtually sampled and are subject to

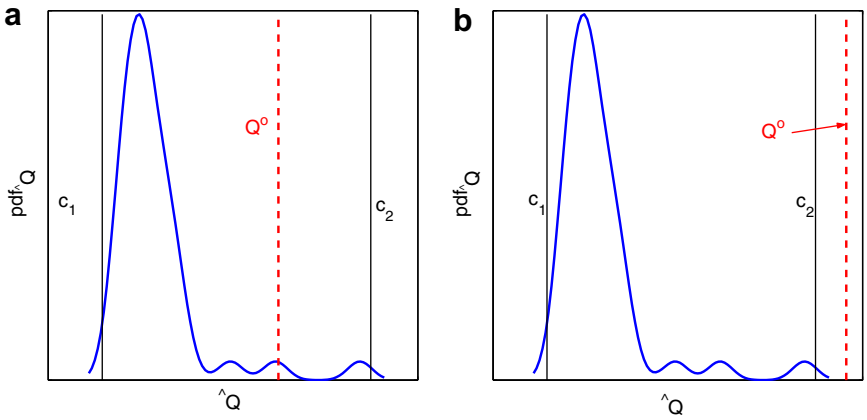

Fig. 1. Possible scenarios for testing H_0 with single observation Q^o. c_1 and c_2 are such that $\text{Prob}(\hat{Q} < c_1) = \text{Prob}(\hat{Q} > c_2) = \frac{\alpha_s}{2}$. (a) No evidence to reject H_0. (b) Reject H_0.

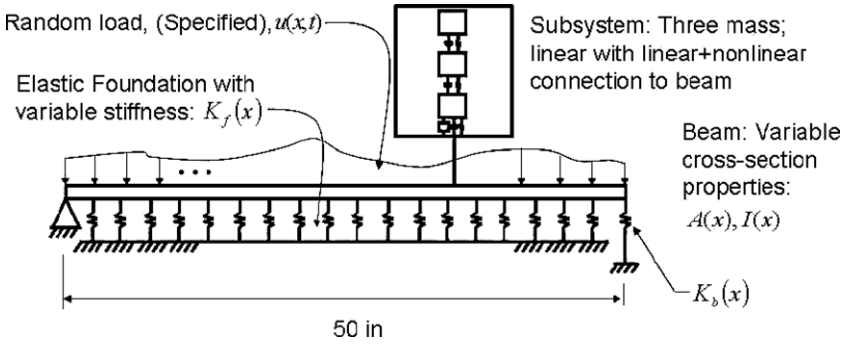

Fig. 2. Target application [38].

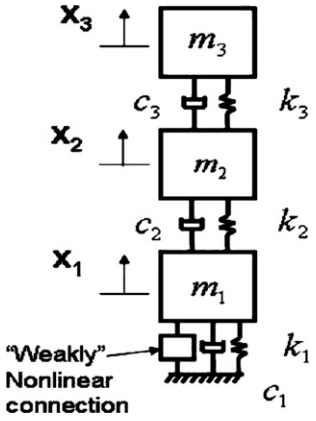

Fig. 3. Subsystem structure [38].

three levels of band-limited Gaussian pseudo white noise applied to mass m_3. For each experiment, the displacement, velocity, and acceleration time histories of masses m_1, m_2, and m_3 are provided. Moreover, for each experiment, modal models are deduced from the response data.

5.3. Subsystem validation

As was the case for the subsystem calibration experiments, 20 nominally identical structures are subject to three levels of shock/decay-free random excitation applied on mass m_3. The idea of having such experiments is to investigate the behavior of the calibrated structure obtained from the calibration experiments under different load conditions. This is clearly justified, since the structure exhibits nonlinearities. Finally, similar sets of outputs as those of calibration experiment are provided.

5.4. Subsystem accreditation

As is the case for most real situations of complex dynamical systems, performing experiments on the original model can be extremely expensive. However, very limited experiments can be carried out on a similar but simpler system. Such system is referred to as the *accreditation configuration* in the present example. The accreditation system consists of a beam with uniform cross-section mounted

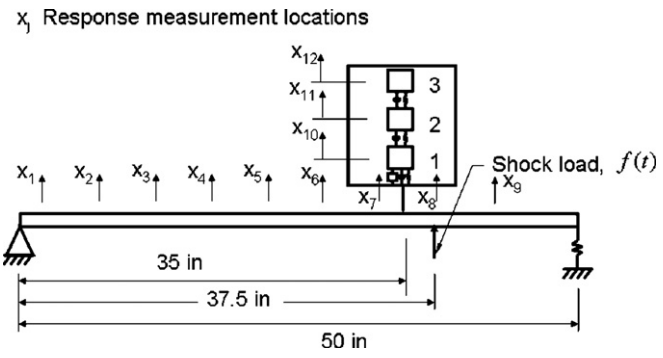

Fig. 4. Accreditation configuration [38].

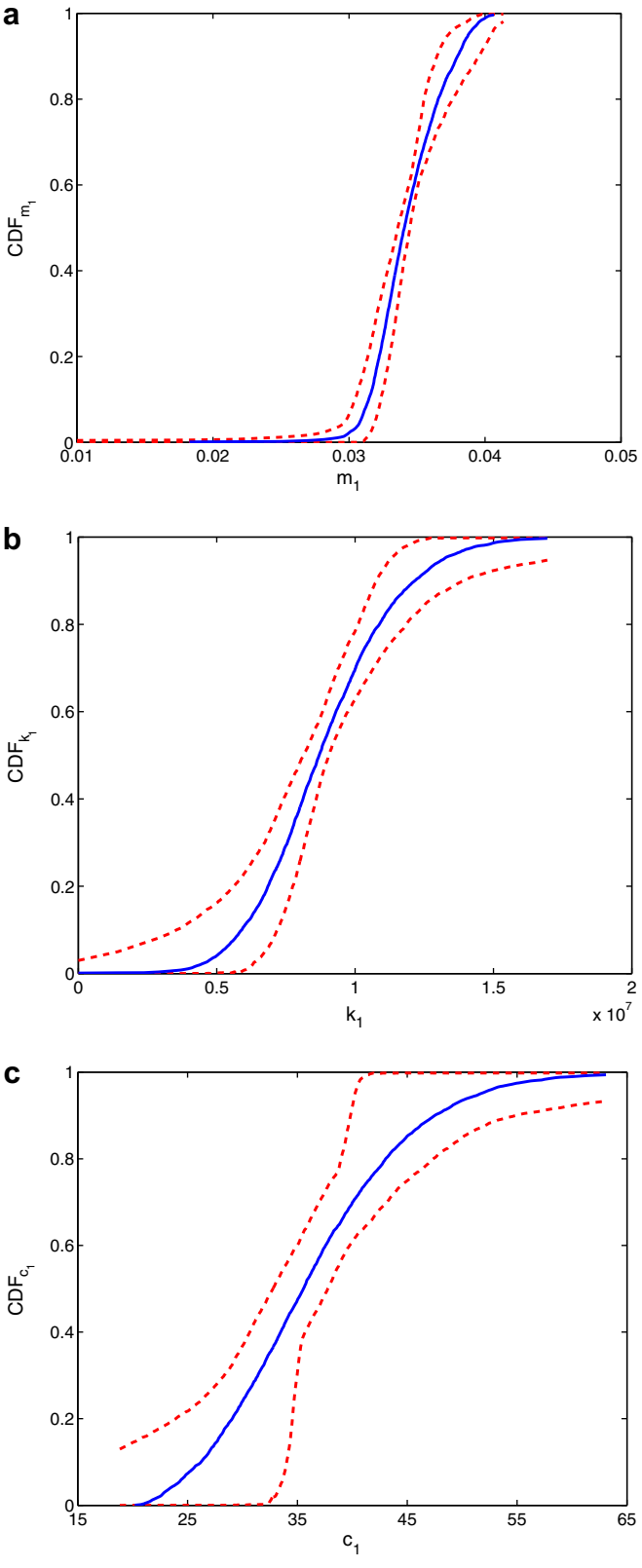

Fig. 5. Probability distribution function of system parameters. Dashed line represents the 95% confidence interval due to epistemic uncertainty: (a) m_1, (b) k_1, and (c) c_1.

on a simple support at one end and on a linear spring at the other end and also the subsystem which is installed on the beam identical to the target application, Fig. 4.

Moreover, the system is excited by a random shock similar to that of the subsystem validation. Since it is expensive to perform experiments on the accreditation configuration, only three experiments are carried out. For each experiment, similar sets of outputs as those of calibration experiment are provided at specific locations on the system, Fig. 4.

As proposed by the problem developers, the mathematical linear model, for all configurations, is the same as the implemented linear model, thus there is no need to perform any model verification for the present problem. Clearly, in situations where there is no such confidence, one should also include the verification step to the validation path.

5.5. Uncertainty representation and propagation

Let $\mathbf{s} := [m_1 m_2 m_3; k_1 k_2 k_3; c_1 c_2 c_3]$ be the vector of parameters of the linear model to be calibrated. It is straightforward to obtain observations of $\mathbf{s}$ given the observation of modal parameters of the subsystem calibration experiments. Consider the following classical equation of motion for the subsystem calibration configuration of Fig. 3

$$\boldsymbol{M}\ddot{\boldsymbol{x}} + \boldsymbol{C}\dot{\boldsymbol{x}} + \boldsymbol{K}\boldsymbol{x} = \boldsymbol{f}, \tag{25}$$

where $\boldsymbol{M}$, $\boldsymbol{K}$, and $\boldsymbol{C}$ are the mass, stiffness, and damping matrices respectively. Let $\boldsymbol{\Phi}$, $\boldsymbol{\omega}$, and $\boldsymbol{\zeta}$ be the mass-normalized matrix of eigenmodes of the system, i.e. $\boldsymbol{\Phi}^t M \Phi = I_3$, the diagonal matrix of modal frequencies, and the diagonal matrix of the modal damping ratios, respectively. Having observations of matrices $\boldsymbol{\Phi}$, $\boldsymbol{\omega}$, and $\boldsymbol{\zeta}$ one can obtain observations of matrices $\boldsymbol{M}$, $\boldsymbol{K}$, and $\boldsymbol{C}$ as

$$\begin{aligned} &\boldsymbol{M} = (\boldsymbol{\Phi}^t)^{-1}\boldsymbol{\Phi}^{-1}; \quad \mathbf{K} = (\boldsymbol{\Phi}^t)^{-1}(\boldsymbol{\omega})\boldsymbol{\Phi}^{-1}; \\ &\mathbf{C} = (\boldsymbol{\Phi}^t)^{-1}(2\boldsymbol{\zeta}\boldsymbol{\omega})\boldsymbol{\Phi}^{-1}, \end{aligned} \tag{26}$$

which then give observations of $\mathbf{s}$. Given 20 observations of $\mathbf{s}$ for each load level of the subsystem calibration data set and based on the procedures proposed in Section 2, the random vector $\mathbf{s}$ is represented as

$$\hat{\boldsymbol{s}} = \bar{\boldsymbol{s}} + \sum_{i=1}^{\mu} \sqrt{\lambda_i} \left(\sum_{j=1}^{p} \tilde{\gamma}_j^{(i)} \bar{\psi}_j(\xi_i) \right) \boldsymbol{\phi}_i, \tag{27}$$

where $\{\boldsymbol{\phi}_i\}_{i=1}^{\mu}$ is the set of eigenvectors associated with first μ-largest eigenvalues $\{\lambda_i\}_{i=1}^{\mu}$ of sample covariance matrix of $\boldsymbol{s}$. For all cases of subsystem calibration data, $\mu = 3$ and $p = 4$ were found to be adequate for representation of $\boldsymbol{s}$. The choice of $\mu = 3$ was based on the number of significant

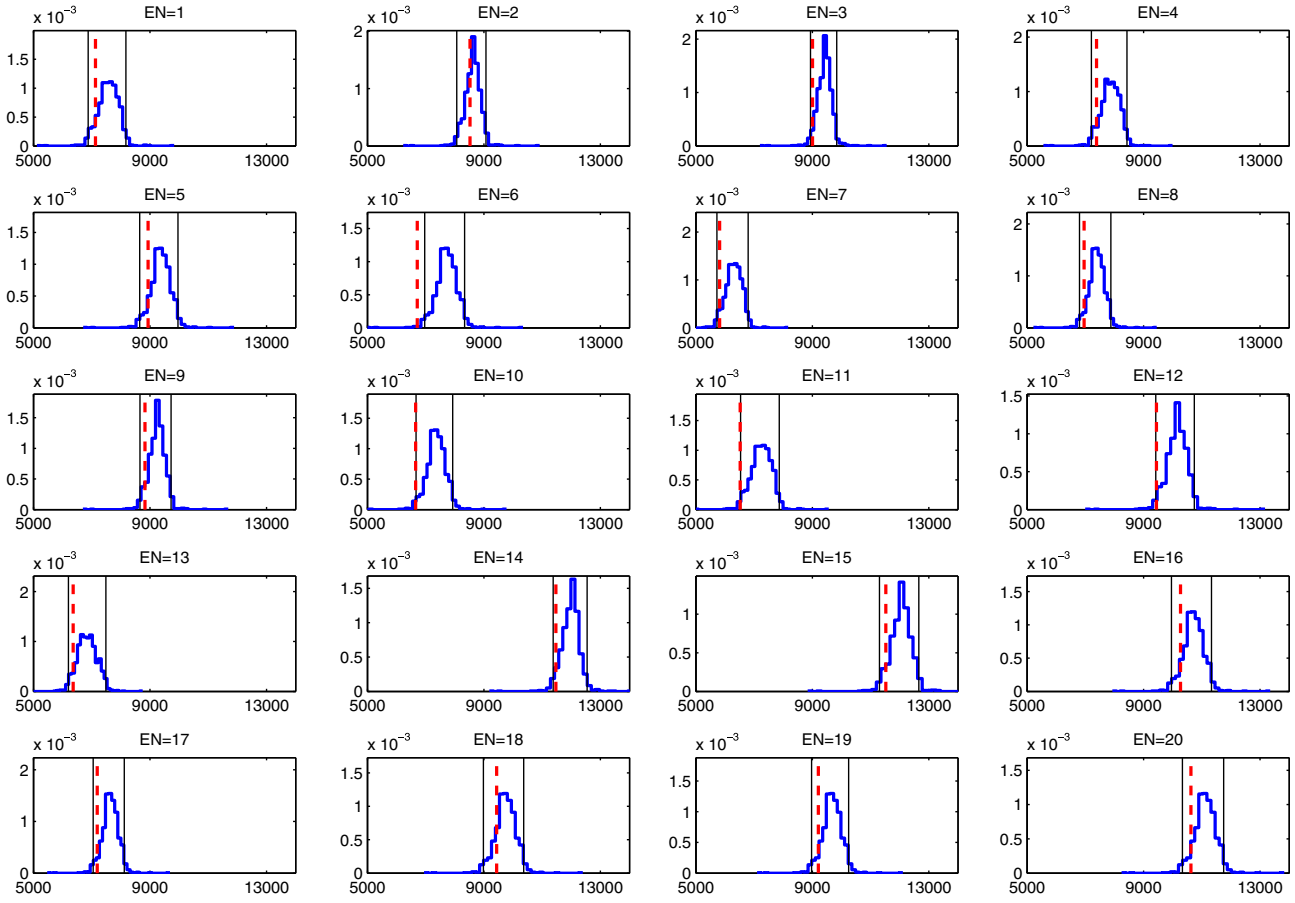

Fig. 6. Hypothesis testing for subsystem validation; calibration-based on low level excitation; validation-based on low level excitation. Horizontal axis represents $\hat{a}_{3m}$ and vertical axis represents $\mathrm{pdf}_{\hat{a}_{3m}}$. *EN* corresponds to the excitation number in the validation data set.

eigenvalues of the sample covariance matrix of $\boldsymbol{s}$. Moreover, a reconstruction based on $p = 5$ has been performed to verify the sufficiency of a 4th order approximation of Eq. (7). For the purpose of illustration, the probability distribution function of m_1, c_1, and k_1 along with the associated variability due to data limitation, epistemic uncertainty, are depicted in Fig. 5. The above results correspond to the case of low level excitation in the subsystem calibration experiments. Such representations were also obtained for all elements of $\boldsymbol{s}$ under all excitation levels.

5.6. Validation metric and prediction–observation comparison

Since the subsystem calibration is performed under three different excitation levels, the whole validation procedure should be repeated once for each calibrated model. More specifically, for both subsystem validation and accreditation configuration, each calibrated model should be subjected to all excitation force levels. Given the regulatory condition, Eq. (24), it is reasonable to assume the maximum acceleration of the top mass in the subsystem, a_{3m}, as the quantity of interest. The predictions of a_{3m}, namely $\hat{a}_{3m}$, are then to be compared with the corresponding experimental observation a^{o}_{3m}.

It is important to note that the quantity of interest plays an important role in the model validation process and it should be related to the intended application of the model. The validity of a candidate model might be rejected for a particular quantity of interest, while at the same time it cannot be rejected for others.

Typical results of the above validation exercise are illustrated in Fig. 6 and are summarized in Tables 1 and 2. It is worth emphasizing that in the present study, a model is rejected when more than 10%, i.e. 2, of the hypothesis tests are rejected. As is observed from these Tables, given the experimental observations, there is not enough evidence to reject the validity of the linear model for prediction of the quantity of interest. Thus one can proceed with the calibrated linear model in order to check the regulatory condition Eq. (24). In Table 3 we show the outcomes of such analyses based on 25 simulations, which strongly suggests that the given design does not comply with the regularity condition of Eq. (24).

Table 1
Subsystem validation analysis

Calibration excitation	Validation excitation	H_0
Low	Low	Accepted
	Medium	Accepted
	High	Accepted
Medium	Low	Accepted
	Medium	Accepted
	High	Accepted
High	Low	Accepted
	Medium	Accepted
	High	Accepted

Table 2
Accreditation configuration analysis

Calibration excitation	Accreditation excitation	H_0
Low	1	Accepted
	2	Accepted
	3	Accepted
Medium	1	Accepted
	2	Accepted
	3	Accepted
High	1	Accepted
	2	Accepted
	3	Accepted

Table 3
Prediction of $P_{a_{3m}} := \mathrm{Prob}\{\max_{t>0}|a(t)| > 1.8(10^4)\ \mathrm{in/sec}^2\}$ based on 25 simulations

Calibration excitation	Sample mean of $P_{a_{3m}}$	Sample variance of $P_{a_{3m}}$
Low	0.0835	0.00083
Medium	0.0662	0.00150
High	0.1269	0.00430

6. Concluding remarks

We have presented a function analytic uncertainty representation using polynomial chaos expansions. This representation is unique in that it provides a sufficiently general context for modeling and analyzing systems possessing both inherent and reducible uncertainties.

We then used this representation for a specific set of structural dynamics systems comprising an idealized model validation exercise. In the course of model validation, one commonly encounters the two classes of uncertainty. While epistemic uncertainty is present in the proposed virtual physics, it was found to have a relatively small effect on predictions. We thus focused our energies on the representation of the parametric uncertainty, where, in contrast to traditional probabilistic approaches, no specific forms for the associated probability distribution functions were assumed. We note that any of the assumptions made in the course of performing the accompanying analyses could have been relaxed using the representation we have proposed.

With our probabilistic constructions in hand, we addressed specific validation questions as traditional statistical hypothesis tests using a simple validation metric. For the case of multiple quantities of interest, more efficient validation criteria will be needed. Based on the available information from the experimental data for the system, the calibrated linear model is found to be adequate to predict the response quantity of interest, which was the maximum acceleration of the top mass in the subsystem, both for the subsystem and accreditation configurations. However, using the validated model, we established that the configuration of the original system did not satisfy the required regulatory condition.

Acknowledgements

Various parts of this work were supported by ONR, NSF and Sandia National Laboratories. Sandia is a multiprogram laboratory operated by Sandia Corporation, a Lockheed Martin Company, for the United States Department of Energy's National Nuclear Security Administration under contract DE-AC04-94AL85000.

References

[1] M. Abramowitz, I.A. Stegun (Eds.), Handbook of Mathematical Functions, ninth printing., Dover Publications, Inc., New York, 1970.
[2] I. Babuška, K. Liu, R. Tempone, Solving stochastic partial differential equations based on the experimental data, Math. Models Methods Appl. Sci. 13 (3) (2003).
[3] I. Babuška, R. Tempone, G. Zouraris, Galerkin finite element approximations of stochastic elliptic partial differential equations, SIAM J. Numer. Anal. 42 (2) (2004) 800–825.
[4] V. Černy, A thermodynamical approach to the traveling salesman problem: an efficient simulation algorithm, J. Optimiz. Theory Appl. 45 (1985) 41–51.
[5] B. Debusschere, H. Najm, P. Pebay, O. Knio, R. Ghanem, O. Le Maitre, Numerical challenges in the use of polynomial chaos representations for stochastic processes, SIAM J. Sci. Comput. 26 (2) (2004) 698–719.
[6] C. Descelliers, R. Ghanem, C. Soize, Maximum likelihood estimation of stochastic chaos representation from experimental data, Int. J. Numer. Methods Engrg. 66 (6) (2006) 978–1001.
[7] DoD. Verification, Validation, and Accreditation (VV&A) recommended practices guide. Technical report, Defense Modeling and Simulation Office, Office of the Director of Defense Research and Engineering, 1996. www.dmso.mil/docslib.
[8] K.T. Fang, R.Z. Li, Some methods for generating both an NT-net and the uniform distribution on a Stiefel manifold and their applications, Comput. Stat. Data Anal. 24 (1997) 29–46.
[9] A. Gelman, J.B. Carlin, H.S. Stern, D.B. Rubin, Bayesian Data Analysis, second ed., Chapman & Hall, Boca Raton, 2003.
[10] R. Ghanem, Probabilistic characterization of transport in heterogeneous porous media, Comput. Methods Appl. Mech. Engrg. 158 (3–4) (1998).
[11] R. Ghanem, Scales of fluctuation and the propagation of uncertainty in random porous media, Water Resour. Res. 34 (9) (1998) 2123–2136.
[12] R. Ghanem, Ingredients for a general purpose stochastic finite elements formulation, Comput. Methods Appl. Mech. Engrg. 168 (1–4) (1999) 19–34.
[13] R. Ghanem, The nonlinear gaussian spectrum of lognormal stochastic processes and variables, ASME J. Appl. Mech. 66 (4) (1999) 964–973.
[14] R. Ghanem, S. Dham, Stochastic finite element analysis for multiphase flow in heterogeneous porous media, Transport Porous Med. 32 (1998) 239–262.
[15] R. Ghanem, A. Doostan, On the construction and analysis of stochastic models: characterization and propagation of the errors associated with limited data, J. Comp. Phys. 217 (1) (2006) 63–81.
[16] R. Ghanem, A. Sarkar, Mid-frequency structural dynamics with parameter uncertainty, Comput. Methods Appl. Mech. Engrg. 191 (2002) 5499–5513.
[17] R. Ghanem, A. Sarkar, Reduced models for the medium-frequency dynamics of stochastic systems, JASA 113 (2) (2003) 834–846.
[18] R. Ghanem, P. Spanos, Stochastic Finite Elements: A Spectral Approach, Dover, 2002.
[19] L. Guadagnini, A. Guadagnini, D.M. Tartakovsky, Probabilistic reconstruction of geologic facies, J. Hydrol. 294 (2004) 57–67.
[20] P. Hall, The Bootstrap and Edgeworth Expansion, Springer-Verlag, 1992.
[21] Allen Hatcher, Algebraic Topology, Cambridge University Press, 2002.
[22] R.G. Hills, T.G. Trucano, Statistical validation of engineering and scientific models: Background. Technical report, Sandia National Laboratories, SAND99-1256, Albuquerque, NM, 1999.
[23] S. Kirkpatrick, C.D. Gelatt, M.P. Vecchi, Optimization by simulated annealing, Science 220 (4598) (1983) 671–680.
[24] A.N. Kolmogorov, S.V. Fomin, Elements of the Theory of Functions and Functional Analysis, Dover Publications, Mineola, NY, 1957.
[25] O.P. Le Maitre, H. Najm, R. Ghanem, O. Knio, Multi-resolution analysis of Wiener-type uncertainty propagation schemes, J. Comp. Phys. 197 (2) (2004) 502–531.
[26] O.P. Le Maitre, O. Knio, H. Najm, R. Ghanem, Uncertainty propagation using Wiener-Haar expansions, J. Comp. Phys. 197 (2004) 28–57.
[27] M. Loeve, Probability Theory, fourth ed., Springer-Verlag, New York, 1977.
[28] S. Mahadevan, R. Rebba, Validation of reliability computational models using Bayes networks, Reliab. Engrg. Syst. Safety 87 (2) (2005) 223–232.
[29] O. Le Maitre, Knio, M. Reagan, H. Najm, R. Ghanem, A stochastic projection method for fluid flow. I: basic formulation, J. Comp. Phys. 173 (2001) 481–511.
[30] G.J. McLachlan, T. Krishnan, The EM Algorithm and Extensions, Wiley, 1997.
[31] I. Meilijson, A fast improvement to the EM algorithm on its own terms, J.R. Statist. Soc., Ser. B 51 (1989) 127–138.
[32] W.L. Oberkampf, M.F. Barone, Measures of agreement between computation and experiment: validation metrics, J. Comp. Phys. 217 (1) (2006) 5–36.
[33] W.L. Oberkampf, T.G. Trucano, Verification and validation in computational fluid mechanics, Progress Aaerospace Sci. 38 (2002) 209–272.
[34] A. Papoulis, Probability, Random Variables and Stochastic Process, McGraw-Hill, 1991.
[35] H. Poor, Introduction to Signal Detection and Estimation, second ed., Springer-Verlag, New York, 1994.
[36] B. Puig, C. Poirion, C. Soize, Non-Gaussian simulation using Hermite polynomial expansion: convergences and algorithms, Probabilist. Engrg. Mech. 17 (2002) 253–264.
[37] J.R. Red-Horse, A.S. Benjamin, A probabilistic approach to uncertainty quantification with limited information, Reliab. Engrg. Syst. Safety 85 (2004) 183–190.
[38] J.R. Red-Horse, T.L. Paez, Sandia National Laboratories validation workshop: structural dynamics application, May 2006. Personal communication and http://www.esc.sandia.gov/VCWwebsite/vcwhome.html.
[39] P.J. Roache, Verification and Validation in Computational Science and Engineering, Hermosa Publisher, Albuquerque, NM, 1998.
[40] S. Sakamoto, R. Ghanem, Polynomial chaos decomposition for the simulation of non-Gaussian non-stationary stochastic processes, ASCE J. Engrg. Mech. 128 (2) (2002) 190–201.
[41] W.A. Scott, Maximum likelihood estimation using the empirical Fisher information matrix, J. Statist. Comput. Simulat. 72 (8) (2002) 599–611.
[42] J. Spall, Introduction to Stochastic Search and Optimization, John Wiley & Sons, 2003.
[43] B. Efronand, R. Tibshirani, An Introduction to the Bootstrap, Chapman & Hall, 1993.
[44] D. Xiu, G. Karniadakis, Modeling uncertainty in flow simulations via generalized polynomial chaos, J. Comp. Phys. 187 (1) (2003) 137–167.
[45] D. Xiu, D.M. Tartakovsky, A two-scale nonperturbative approach to uncertainty analysis of diffusion in random composites, J. Multiscale Model. Simulat. 2 (4) (2004) 662–674.
[46] N. Young, An Introduction to Hilbert Space, Cambridge University Press, Cambridge, UK, 1997.
[47] R. Zhang, S. Mahadevan, Bayesian methodology for reliability model acceptance, Reliab. Engrg. Syst. Safety 80 (1) (2003) 95–103.